THE ASTROPHYSICAL JOURNAL, 486:1006–1012, 1997 September 10

THE ULTRAVIOLET SPECTRUM OF THE MAGNETIC CATACLYSMIC VARIABLE RX J1802.1+1804

C. R. SHRADER[1,2]
Laboratory for High Energy Astrophysics, NASA Goddard Space Flight Center, Greenbelt, MD 20771;
shrader@grossc.gsfc.nasa.gov

K. P. SINGH
X-Ray and Gamma-Ray Astronomy Group, Tata Institute of Fundamental Research, Mumbai, India 400005;
singh@tifrvax.tifr.res.in

AND

P. BARRETT[1]
Laboratory for High Energy Astrophysics, NASA Goddard Space Flight Center, Greenbelt, MD 20771;
barrett@compass.gsfc.nasa.gov
Received 1996 October 23; accepted 1997 April 10

ABSTRACT

We observed the counterpart to the X-ray source RX J1802.1+1804, an object recently discovered as part of a survey to identify the optical counterparts to ultrasoft X-ray sources in the *ROSAT* point-source catalog that was subsequently identified as a magnetic cataclysmic variable, with the ultraviolet spectrometers on *IUE* in low dispersion mode. We report on the results of these observations and interpret our data within the context of other UV spectroscopic studies of magnetic CVs (polars). RX J1802.1+1804 is a relatively bright UV source, with a UV-to-optical flux ratio and emission-line spectrum similar to other well-studied CVs. Our observations insufficiently sample the binary orbit to discern any phase-dependent effects. We found RX J1802.1+1804 to have an unusually large He II λ2733 emission-line strength, and we have also made probable detections of weaker He II lines at 2511, 3203, and possibly 2386 Å, in addition to the more commonly detected He II at 1640 Å. We suggest that RX J1802.1+1804 is thus anomalous in terms of its overall He II emission-line spectrum among the sample. Several lines of O III $\lambda\lambda$3047 and 3133 are apparently detected as well, which is unusual for CVs at the signal-to-noise ratio levels obtainable with *IUE* long-wavelength spectrograph. Given the seemingly rich spectrum of helium and oxygen emission lines, and the known relationship between He II Lyα and the oxygen lines, i.e., the Bowen fluorescence mechanism, we can, in principle, constrain the size and thermodynamics of the emitting region. This analysis suggests that $R \sim 10^9$ cm and $n_e \sim 10^{11}$ cm^{-3}. This physical scale is consistent with the line-emission originating in the accretion column rather than in a hot spot on the white dwarf surface.

Subject headings: novae, cataclysmic variables — stars: individual (RX J1802.1+1804) — ultraviolet: stars

1. INTRODUCTION

The X-ray source, RX J1802.1+1804, was discovered as part of a compilation of "ultrasoft" X-ray sources from the *ROSAT* WGACAT Catalog (Singh et al. 1995b; White, Giommi, & Angelini 1994). The large softness ratio and pronounced variability of the X-ray source are characteristic of the polar subclass of magnetic cataclysmic variables (mCVs), also commonly known as AM Herculis binaries or "polars." These close binaries (reviewed in, e.g., Cropper 1990; Beuermann et al. 1996) contain white dwarfs with a magnetic field strength sufficiently strong (15–70 MG) to synchronize the rotation and orbital periods, and to divert the accreting material away from the orbital plane and toward the magnetic poles. Optical follow-up observations (Szkody et al. 1995) showed many of the characteristics of the polar subclass: He II strength greater than Hβ, multiple line components, circular polarization, and a consistent photometic, polarimetric, spectroscopic, and X-ray period of 113 minutes. We also note that the 113 minute period puts RX J1802.1+1804 just below the period gap where over half of all polars are found.

The ultraviolet spectra of polars typically show a strong blue continuum and strong emission lines of C IV λ1550, N V λ1240, Si V λ1397, He II $\lambda\lambda$1640, 2733, and Mg II λ2800 in the high state. Lower ionization states of C III λ1175, C II λ1335, N IV λ1718, and Si II λ1300 are also sometimes present, and polars seem to have a broader range of ionization than intermediate polars and nonmagnetic CVs. For a recent review of the UV properties of mCVs see de Martino (1995). Emission lines can be a powerful diagnostic of the physical conditions in the ionized material. For example, Mauche, Lee, & Kallman 1997) indicate that the photoionization models reproduce the N V:Si IV:C IV line ratios better than the collisional ionization models, although no model reproduces the observed He II/C IV line ratios. Other important emission lines located in the near-UV are subsets of the He II Balmer and Paschen series, and the O III Bowen lines.

RX J1802.1+1804 has an exceptionally strong, soft X-ray excess component when compared with the currently known polars, have a ratio of blackbody to bremsstrahlung components of 55–120 (Szkody et al. 1995; Greiner, Remillard, & Motch 1995). The large range quoted for this ratio

[1] Also at Universities Space Research Association.
[2] Guest observer, *International Ultraviolet Explorer* operated by NASA Goddard Space Flight Center.

arises from the inability of *ROSAT* PSPC measurements to constrain the bremsstrahlung temperature above 1 keV, and the sensitivity of the blackbody component to the total column density. Typical values of this quantity range from less than 0.1 to ~ 100 with a mean of about 10, where these numbers are based on a sample of 15 polars (Ramsey et al. 1994). Szkody et al. (1995) also argue, based on the apparent correlation between soft X-ray excess and magnetic field strength, that RX J1802.1+1804 is probably a high field strength polar ($B \sim 50$ MG), and thus the accretion column is probably strongly collimated. We use the term high field strength here in a relative sense as evidence for a field strength of $B \sim 230$ MG in one particular mCV, AR UMa, has recently emerged (Schmidt et al. 1996); most polars are believed to have field strengths in the 10–70 MG range.

Knowledge of RX J1802.1+1804 as a strong, soft X-ray and moderately bright ($V = 14.5$ mag) optical source encouraged us to request *IUE* observations of this mCV. We observed the $V = 14.5$ mag optical counterpart to RX J1802.1+1804 with the long and short-wavelength instruments on 1995 August 31. A total of six spectra, two LWP and four SWP, were obtained using the low-resolution modes of the spectrographs, with the goal of determining its UV continuum energy distribution, the galactic extinction along the source line of sight, its emission-line spectrum and, if possible, any gross phase-dependent effects. We found the source to be reasonably UV bright, with an emission-line spectrum that is particularly rich including, for example, apparent detections of multiple lines of helium and carbon in addition to oxygen lines believed to be due to the Bowen fluorescence mechanism.

We summarize our observations and data analysis in § 2 and list our detected lines in Table 2 below. In § 3, we present an analysis of the UV spectra of a sample of polars obtained from the NASA *IUE* data archive to highlight some properties of the RX J1802.1+1804 spectrum within a statistical context. In § 4, we discuss possible constraints on the physical conditions within the emission-line region that can be inferred from our data, both from consideration of the He II line spectrum and the Bowen fluorescence mechanism. Some conclusions are drawn in § 5.

2. OBSERVATIONS AND DATA ANALYSIS

2.1. *Observations*

The discovery of RX J1802.1+1803 was announced on 1995 August 1 (Singh et al. 1995a; Greiner et al. 1995), which was subsequent to the application period for the final *IUE* observing proposal cycle, and within months of the termination of *IUE* Science Operations at the NASA Goddard Space Flight Center. Its visual magnitude, $V \approx 14.5$, places it among the four or five brightest polars known, and as such, study with the *IUE* low-dispersion spectrographs was plausible. We thus requested and were awarded director's discretionary time to obtain a set of spectra. Since at the time of the observations we were largely ignorant of its intrinsic UV brightness, and of any possible galactic extinction, we first obtained an LWP test exposure of 40 minutes duration. We found that the source to be relatively UV bright suffering no apparent galactic extinction. Unfortunately, no strictly simultaneous visual photometric measurements were made, but visual photometry and spectroscopy several nights earlier, and at several other times during the preceding 1.5 months were consistent with a $V \approx 14.5$ source. Based on this, its UV-to-visual flux ratio is about 1.6 times that of AM Her, and above, but within a standard deviation, of the mean for the *IUE* mCV sample we discuss in § 3. No contamination from solar light scattered into the telescope tube, as has often been a problem for *IUE* observations within certain Sun-angle ranges since about 1991 (Carini, Weinstein, & Walker 1993), was apparent here in as far as acquisition and tracking could be affected; however, we were not able to obtain any useful photometric information from *IUE*'s fine error sensor (FES) as the target was too faint relative to the scattered-light background. Acquisition was accomplished using a "blind-offset" technique. Although the absolute target positioning within the $10'' \times 20''$ large aperture was initially off by several arcseconds because of some combination of coordinate error in the offset star, the target, or error in the acquisition maneuver, it was well within the aperture. In any case, it was displaced primarily in a direction perpendicular to the dispersion axis, thus the absolute flux and wavelength calibration are believed to be valid. A guide star was clearly detected with the FES at a level of greater than 120 counts above background, thus allowing subarcsecond positional accuracy (i.e., repeatability) for subsequent repositioning of the target. We used the raw-flux measurement obtained in real time from this initial LWP exposure to scale exposure times for subsequent SWP. An additional LWP was obtained in parallel with SWP readout overhead time as well. A log of our observations is presented in Table 1.

2.2. *Data Reduction*

Each spectrum was processed by the "NEWSIPS" system, which was by that time the standard processing system at the NASA *IUE* Observatory Data Analysis Center (IUEDAC) (Nichols et al. 1994). Additionally, we performed a Gaussian re-extraction of the standard line-by-line data products for comparison purposes and examined carefully the raw spectrograph images for the charged particle events that could lead to the appearance of spurious features in the data. Subsequent analysis was performed

TABLE 1

LOG OF OBSERVATIONS

Instrument	Image Number	TJD Start	UT Date	UT Start Time	Exposure (minutes)	Phase Interval
LWP	31382	9960.578	1995 Aug 31	02:11:59	40	0.37–0.90
	31383	9960.649	1995 Aug 31	03:59:06	25	0.04–0.62
	31383	9960.704	1995 Aug 31	05:43:19	25	0.33–0.55
SWP	55773	9960.618	1995 Aug 31	03:04:06	40	0.92–0.27
	55774	9960.669	1995 Aug 31	04:33:04	60	0.71–0.24
	55775	9960.765	1995 Aug 31	06:20:58	60	0.66–0.19
	55776	9960.808	1995 Aug 31	07:52:59	60	0.48–0.00

using the standard IUEDAC analysis software. Comparison of the four SWP spectra revealed no gross differences in shape or intensity level. We thus performed a co-addition of all four spectra to optimize line identifications and construct a phase-averaged continuum energy distribution. The resulting spectrum is illustrated in Figure 1*a*. A co-addition of our two LWP spectra is shown in Figure 1*b*.

Immediately evident was the lack of any gross continuum structure, such as a pronounced far-UV excess, as seen for example in AM Her during certain phase intervals (Beuermann et al. 1996; Raymond et al. 1979). Despite the fact that RXJ 1802.1+1804 has a pronounced soft excess, much more so than AM Her, for example (Szkody et al. 1995; Ramsey et al. 1994), a blackbody fit to the *ROSAT* PSPC data strongly suggests that the X-rays cut off too sharply at low energies ($T_{BB} \approx 20$–45 eV) to be associated with the UV, which is approximated by a flat ($f_\lambda \propto \lambda^{-0.3}$) power law (in any case, the phasing of the UV steepening and the soft X-ray excess in AM Her seem to be inconsistent with a common thermal origin [e.g., Heise & Verbunt 1988]). The flux per decade (νF_ν) is thus decreasing with frequency resembling EF Eri, for which the soft–X-ray excess and the UV continuum are clearly separate components In AM Her, on the other hand, the phase-averaged $\nu - \nu f_\nu$ spectral energy distribution increases with frequency in the UV, and the UV and soft X-rays may overlap or possibly connect smoothly (Beuermann et al. 1996).

2.3. *Phase-dependent Effects*

Since the required exposure times for either (SWP or LWP) spectrograph are typically $\frac{1}{3}$–$\frac{1}{2}$ of an orbital period, our observations are not "phase resolved" in any reasonable sense. Also, one of our LWP exposures was taken in two 25 minute segments separated by about 1 binary orbital period, thus covering a common, middle, $\frac{1}{3}$-phase interval. We also have distinct coverage of approximately the first quarter-phase interval and the second half–phase interval with the SWP. The binary ephemeris used in our phase analysis was from Greiner et al. (1995) based on their *ROSAT* observations:

$$T(\mathrm{HJD}) = 2{,}448{,}907.26986597 + 0.078498(\pm 0.000115)E\ .$$

Given the width of the phase intervals sampled, and the magnitude of the expected radial velocity shifts (Szkody et al. 1995 measure an Hα radial velocity amplitude of ~ 185 km s^{-1}) and the $\sim 0\farcs5$ uncertainty in positioning of the star in the aperture, clearly no radial velocity information is forthcoming from our observations.

RX J1802.1+1804 exhibits apparent eclipses in its X-ray light curve, where the *ROSAT* PSPC count rates drop to nearly zero intensity at about phase 0.7, and dip to about one-half peak intensity at phase 0.1 (Greiner et al. 1995; Szkody et al. 1995). Additionally, shallow (0.4 mag) dips are seen in the optical light curve. The X-ray eclipsing, combined with the absence of eclipsing in the optical band, has been interpreted by Greiner et al. as the disappearance of the (small) X-ray–emitting region behind the rotating limb of the white dwarf. Other interpretations are possible, but in any case, it seems likely that we may be viewing the system at an inclination of $\sim 65°$–$75°$, which as we will show in § 4. is consistent with our UV line-width measurements considered in the context published statistical studies of CVs relating line widths to viewing geometry.

Three of our SWP integrations include most or all of the phase interval of the X-ray eclipse (Table 1). There is no discernible difference in the UV continuum or line fluxes, however, between the SWP exposure that excludes the X-ray eclipse at phase 0.7 (which is about 15–20 minutes in width) and the others that overlap or include it.

2.3. *Emission-Line Spectrum*

A rich emission-line spectrum dominated by N v λ1240, O i/Si iv $\lambda\lambda$1393, 1402, C iv λ1549, He ii $\lambda\lambda$1640, 2733, and Mg ii λ2800 is evident (Fig. 1; Table 2). These UV line features are seen in numerous other magnetic and nonmagnetic CVs in varying degrees. The measurements listed in Table 2 resulted from the application of an interactive routine to perform an empirical integration over the line profile. Uncertainties were estimated by averaging over residual noise features on the adjacent continuum regions.

The He ii λ2733 feature appears to be unusually strong: it is nearly as strong as the Mg ii λ2800 feature which is rarely found to be the case. The relative strengths of the He ii lines in the LWP band will be discussed further in § 3, possible constraints on the physics of the emitting region from the He ii line spectrum are discussed in § 4. We note that in RX J1802.1+1804 (in both the co-added and the individual spectra), and in the other mCV spectra that we will discuss

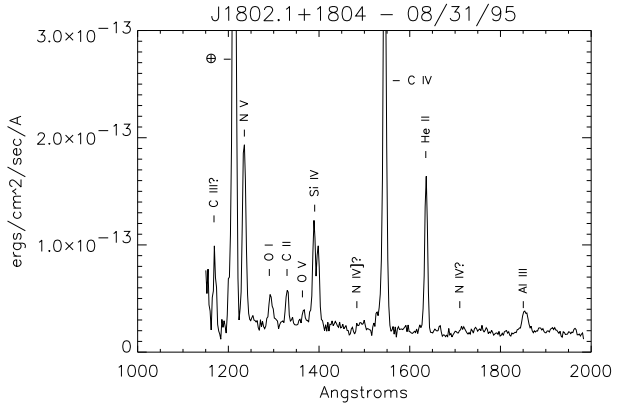

FIG. 1*a*

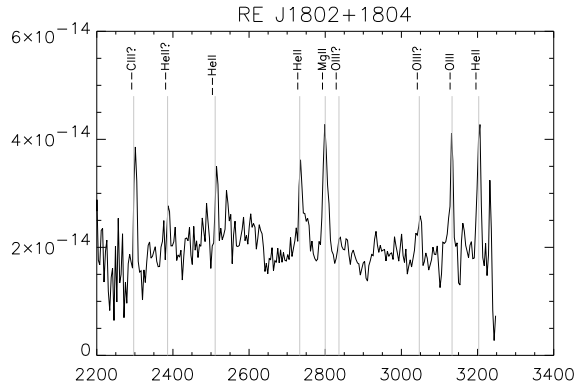

FIG. 1*b*

FIG. 1.—(*a*) SWP Spectrum resulting from the coaddition of four individual SWPs obtained over arbitrary phase intervals. The vertical axis is flux in ergs cm^{-2} s^{-1} and the labels indicate our line identifications. (*b*) LWP Spectrum of RX J1802.1+1804. Note the unusually strong line of He ii λ2733 as well as the apparent presence of He ii $\lambda\lambda$2386, 2511. The Bowen fluorescence lines of O iii $\lambda\lambda$3047, 3133 are also evident. The latter may be blended with O iii λ3123 indicating that multiple branches of the Bowen process are probably occurring.

TABLE 2

OBSERVED UV EMISSION LINES

Ion	λ	EW	σ_{EW}	Flux[a]	σ_F[a]
C III.....	1176	−21.0	−4.8	5.10	0.98
N V	1240	−61.2	−5.1	16.50	1.00
O I/Si III.....	1297/1302	−14.5	−2.9	3.53	0.56
C II	1335	−9.1	−1.3	2.50	0.29
O V	1371	−2.8	−1.0	0.93	0.21
O I/Si IV.....	1393/1402	−46.1	−1.9	12.62	0.50
N IV	1486	−4.9	−2.2	1.05	0.46
C IV.....	1550	−187.9	−2.9	38.42	0.70
He II	1640	−55.1	−1.7	11.28	0.32
N IV	1718	−3.3	−0.9	0.59	0.15
Al III	1856	−20.2	−2.3	3.62	0.40
C II	2297	−15.6	−4.2	2.38	0.63
He II	2386	−8.4	−2.1	1.53	0.47
	2511	−5.3	−1.9	1.12	0.45
	2733	−21.8	−2.0	3.92	0.33
O III	2836	−2.5	−1.4	0.46	0.25
Mg II	2800	−23.2	−2.0	4.08	0.34
O III	3047	−3.9	−1.3	0.68	0.21
	3133	−11.2	−3.0	2.02	0.40
He II	3203	−15.5	−1.8	2.80	0.44

[a] The flux is in units of 10^{-13} ergs cm^{-2} s^{-1}.

in § 3, He II λ2733 appears to be blended on its red wing, probably with Fe II λ2740. We additionally identify the possible detection of another ion of carbon, C III λ2297, which again is in a spectral region of poor sensitivity for the LWP and is in fact near the (blue) threshold of our continuum detection. In addition, we note possible detections of several additional lines identified with He II $\lambda\lambda$2386, 2511, 3204 that are often indiscernible from the noise background inherent in this instrument; this is particularly true for C III λ2297 and He II λ2386 where the LWP sensitivity shortward of 2400 Å is notoriously poor. Also, apparent detections of several of the O III Bowen fluorescence lines ($\lambda\lambda$3047, 3123, 3133) are identified; these are also often undetected in *IUE* spectra, although some previous cases have been reported, most notably in AM Her itself (Raymond et al. 1979). A very marginal feature coincident with an additional Bowen O III line is seen at λ2836, which we note as a line "identification" only because of the presence of the other O III features, and in particular the strength of the λ3133 feature. We also weakly detect the C III 1176 Å line, which is near the extreme blue-end range of the SWP's sensitivity curve.

3. COMPARISON WITH OTHER POLARS

3.1. *Archival Data Analysis*

We obtained spectra from the *IUE* data archive at the National Space Science Data Center for a subsample of the polars that have been studied with *IUE*, using the selection simple selection criteria that both SWP and LWP (LWR) spectra of sufficient quality existed. Our resulting sample and some measured quantities are listed in Table 3. These data were analyzed, in a manner consistent with that applied to our RX J1802.1+1804 spectra, for purposes of a comparison study and to search for possible correlations between UV properties and known properties from measurements at other wavelengths. Typically, three to five individual low-dispersion spectra were wavelength shifted to a common scale and then co-added to achieve optimal signal-to-noise ratio. Data reprocessed using the NEWSIPS system were used wherever possible. The standard set of corrections for instrument sensitivity degradation with time was applied to the older data as appropriate. Data resulting from observations made during low-accretion rate states were avoided; such campaigns were carried out for example in AM Her and BY Cam to study the "bare" white dwarf. We were similarly cautious to avoid eclipse-phase measurements. RX J1802.1+1804 was clearly in a high-accretion state at the time of our observations, and we are ultimately interested in obtaining insight into the physics of the matter in the accretion column, the low-state or eclipse-phase observations were obviously undesirable for drawing comparisons.

3.2. *Statistical Properties*

RX J1802.1+1804 is characterized by an unusually soft X-ray spectrum. One might naively suspect that a relationship exists between the UV characteristics in mCVs and the "softness" parameter, $\zeta \equiv L_{soft}/(L_{cyc} + L_{hard})$ as defined, for example by Ramsey et al. (1994). Some of the lines for example, could presumably be formed in X-ray–heated material near the base of the accretion column with the thermal X-ray emission providing the ionizing flux,

TABLE 3

RELEVANT UV LINE MEASUREMENTS FROM ARCHIVAL OBSERVATIONS

	He II λ1640		He II λ2733		Mg II λ2800	
NAME	EW	Flux[a]	EW	Flux[a]	EW	Flux[a]
RX J1802+18.....	−55.1	11.3	−21.8	3.92	−23.2	4.08
AN UMa	−79.4	2.35	−10.6	0.15	−38.0	0.63
BL Hyi.....	−61.0	2.20	−3.8	0.07	−59.7	1.07
BY Cam	−93.2	13.0	−8.3	0.49	−13.5	0.72
EF Eri	−42.7	7.75	−5.2	0.56	−15.9	1.66
HU Aqr	−37.9	4.11	−11.7	0.31	−20.6	0.56
AM Her	−43.3	31.4	−9.5	0.44	−22.5	10.3
MR Ser	−26.7	4.93	−5.2	0.18	−22.7	0.82
QQ Vul.....	−27.1	5.31	−8.2	1.20	−12.7	1.69
RE J1844−74.....	−27.7	1.33	−12.4	0.49	−51.6	1.31
RE J1938−46.....	−40.2	5.04	−1.9	0.19	−14.9	1.82
RX J0515+01.....	−52.9	2.96	−12.6	0.50	−13.9	0.48
V2301 Oph	−27.6	1.38	−3.0	0.10	−34.1	1.18
V834 Cen	−28.5	4.36	−15.9	1.01	−28.9	1.74
VV Pup.....	−100.2	9.68	−1.5	0.01	−50.1	1.10

[a] The flux is in units of 10^{-13} ergs cm^{-2} s^{-1}.

although more complex scenarios invoking multiple emitting regions at multiple temperatures are probably more realistic. Among our sample, RX J1802.1+1804 has the highest softness parameter, $\zeta \sim 10^2$, as noted by Szkody et al. (1995). It is also notable among the UV sample for its rich emission-line spectrum, although it does not exhibit unusually strong emission lines of the most commonly detected species; N v, Si iv, C iv, He ii, Mg ii. In terms of the integrated UV line-to-continuum luminosity, which as noted by Bonnet-Bidaud & Mouchet (1989) is higher in magnetic than in nonmagnetic CVs, RX J1802.1+1804 has very nearly the median value among our sample objects. The line-flux ratios, log Si iv/C iv ≈ -0.53, and log N v/C iv ≈ -0.37 are very similar to the median values, among mCVs as well as other CV subclasses, as defined by Mauche et al. (1997), although there seems to be some systematic shift between the measurements of those authors and of de Martino (1995). For the latter, our measurements lie more near the edge of the polar sample.

Among the UV sample, RX J1802.1+1804 is notable, however, for the strength of the He ii λ2733 line, which is comparable to that of the adjacent Mg ii λ2800 feature: both reside on a portion of the LWP instrument where its sensitivity is nearly optimal. Figure 2 illustrates the He ii λ2733 to Mg ii λ2800 versus He ii λ1640 to He ii λ2733 intensity ratio for the UV sample. RX J1802.1+1804 also has the second highest He ii 2733 Å line strength relative to the stronger He ii 1640 Å (He ii Hα) line among the sample ($\sim$0.3); the expected ratio for recombination is $\sim$0.1. Other He ii lines, such as λ3204 (He ii Hγ) are detected in only a small subset of the sample. In the data we examined, only in AM Her itself were each of the He ii λ2511 and λ3204, as well as O iii λ3133 lines evident. As an illustration of the relative strengths of these lines, we have plotted the near-UV spectra of RX J1802.1+1804 overlying the same portion of a representative AM Her spectra (Fig. 3). In Figure 3, RX J1802.1+1804 has been scaled to have nearly the same continuum level as AM Her. The AM Her spectra is based on a coaddition of four archival spectra. Note that while Mg ii λ2800 is nearly identical for the two sources, the He ii $\lambda\lambda$2511, 2733, and 3204 features, as well as O iii $\lambda\lambda$3047 and 3133 appear to be much stronger in RX J1802.1+1804.

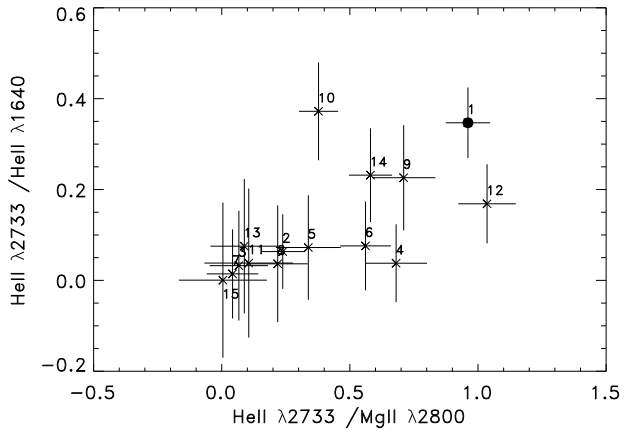

FIG. 2.—Line ratios He ii λ2733 to Mg ii λ2800 vs. He ii λ1640 to λ2733 distribution for a sample of UV-bright polars accessible to *IUE*. The sources are (1) RX J1802.1+1804, (2) AN UMa, (3) BL Hyi, (4) BY Cam, (5) EF Eri, (6) HU Aqr, (7) AM Her, (8) MR Ser, (9) QQ Vul, (10) RE 1844−74, (11) RE 1938−461, (12) RX 0515+01, (13) V2301 Oph, (14) V834 Cen, and (15) VV Pup.

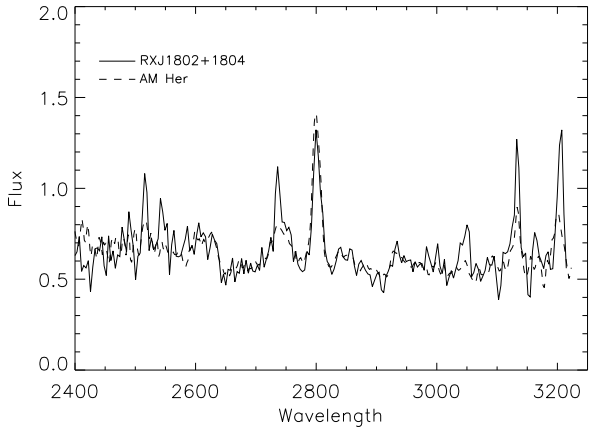

FIG. 3.—A Portion of the LWP spectrum of RX J1802.1+1804 (*solid line plot*) overlying a similar portion of a spectrum of AM Her (*dashed line plot*) resulting from the coaddition of several archival spectra. The RX J1802.1+1804 spectrum has been scaled to the approximate level of Am Her and scaled by 10^{13} ergs cm^{-2} s^{-1}. Note that while the Mg ii λ2800 features are very similar, the He ii $\lambda\lambda$2511, 2733, 3203 and the O iii $\lambda\lambda$3037, 3133 seem to be significantly stronger in RX J1802.1+1804.

No distinct correlations were found between the softness parameter and individual line strengths, or with integrated UV line-to-continuum ratios. These quantities might naively be expected to be related to ζ if the UV and soft X-rays emanate from the same region. Recent evidence, however, suggests that the different continuum components and the UV lines come from distinct regions. In a phased-resolved spectroscopic study of ST Lmi and UZ For, for example, Stockman & Schimdt (1996) have shown that a small hot spot, perhaps at the base of the impact stream is the likely site of the soft X-ray and far-UV emission (as well as the cyclotron component), while the UV lines seem to be emitted from the accretion column possibly extending all the way to the L_1 point. In any case, the wide range of ionization levels in mCVs is indicative of multiple temperature regions. There does appear to be correlation between softness and the He ii λ2733:λ1640 line-flux ratio (Fig. 4). This seems peculiar, as this ratio is indicative of a higher density of absorbing material, contrary to the expected low ambient gas density expected to characterize

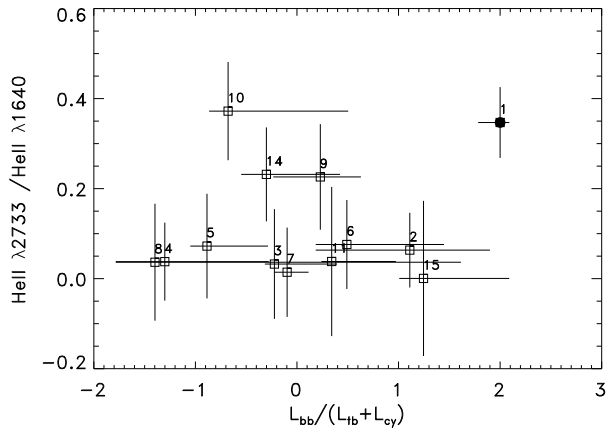

FIG. 4.—X-ray "softness" parameter $\zeta \equiv L_{soft}/(L_{cyc} + L_h)$ vs. the He ii λ2733:λ1640 line ratio for 13 UV-bright polars. The numerical lables used are the same as in Table 3 and Fig. 2. Values of ζ are from Ramsey et al. (1994), except for RX J1802.1+1804, which we measured.

the environment of the ultrasoft X-ray sources. This suggests, for example, that these lines may arise from dense blobs of accreting matter characterized by small filling factors. Such blobs could exist at the base of the accretion column.

A complete understanding of the temperature, ionization state, density, elemental abundance, and geometrical distribution of the gas emitting the UV lines would require the application of detailed photoionization codes as has been attempted, for example, in the domain of AGN studies. Recently, such an effort undertaken by Mauche et al. (1997) on an ensemble of CVs using line-flux ratios for the principle lines of N v, Si iv, C iv, and He ii and assuming different input models for the ionizing radiation spectrum represents in our view perhaps the most comprehensive effort to date—yet it has met with limited success. The only model that came close to matching the observed line-flux ratios was the one based on a very soft blackbody with $kT = 10$ eV. As previously noted, our line-flux ratios for RX J1802.1+1804 are contained well within the range of values of mCV measurements presented by those authors, so this type of model would likely have similar success for this source. What is unusual in RX J1802.1+1804 is the strength of the He ii 2733 Å, which was not considered by Mauche et al. (1997). Below we discuss the He ii line spectrum and attempt to derive some physical parameters from an analysis of the Bowen fluorescence line spectrum.

4. DISCUSSION

4.1. He ii *Line Spectrum*

We can compare the flux ratios of the detected Balmer and Paschen series He ii lines with the expected ratios for a recombination spectrum. Deviations are indicative of optical depth effects, and a certain amount of information can, in principle, be inferred. Following the approach of Stockman et al. (1977), with modifications suggested by Schachter et al. (1991), and using a simple slab model, we can compare the observed He ii line-flux ratios with the predicted values under the assumption that the individual line optical depths are large, and that the plasma satisfies LTE. We fitted the observed line-flux ratios to a model of the form $F = B_\nu(T)[1 - \exp(-\tau)]\Delta\nu$, where τ is the line opacity and different τ_i (the indices refer to different transitions) are related by the relative line strengths (oscillator strengths) f_i. Temperature (T) and optical depth are varied as free parameters in a least-squares fitting procedure leading to a parameter-space "goodness of fit" grid: contours, corresponding to confidence levels of 68% and 90% were constructed From this analysis, we find the best-fit values, for ratios such as He iiγ/He ii and He iiδ/He iiγ, corresponding to about $T \approx 31{,}000$ K and $\tau_{1640} \approx 15$—we must emphasize here, however, that although the 90% confidence contours allow for a wide range in these parameters, the contours fail to close for the full range of reasonable temperatures, from 10,000 to 40,000 K.

4.2. *Bowen Fluorescence Lines*

We have made apparent detections of the O iii lines at 3047 and 3133 Å believed to be due to the Bowen fluorescence mechanism; a possible but very marginal detection of O iii λ2836 is also evident (Fig. 2). The λ3133 feature is apparently blended with yet another Bowen line at 3123 Å (Fig. 5). Attempts to deblend the two components, leading

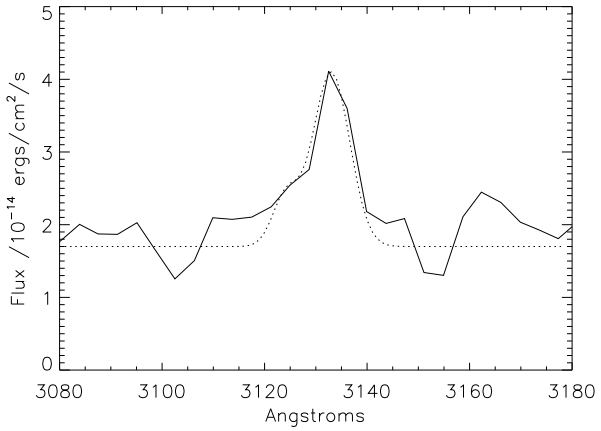

FIG. 5.—O iii $\lambda\lambda$3123, 3133 Bowen fluorescence feature. The 3133 Å line is dominant, but a Gaussian-deblending fit to the total profile (*dotted-line curve*) is suggestive that the 3123 Å line is indeed present.

to the fit illustrated in Figure 5, suggest that the λ3123 feature contributes $\sim$15% of the total flux, consistent with the predicted value of 10% (Kastner & Bhatia 1996). Detection of the 3123 Å line, which seems to be the case here, is a clear indication that the Bowen O3 process is operating in addition to the O1 process. Applying a correction factor to account approximately for the λ3123 contribution we obtain a ratio of the O iii λ3133:λ3047:λ2836 of 1.0:0.35:0.25. Given the considerable uncertainty of the λ3047 and particularly the λ2836 features, this result is consistent with the theoretical values of 1.0:0.18:0.10. (e.g., Osterbrock 1989) or 1.0:0.19:0.12 (Kastner & Bhatia 1996).

Since the Bowen mechanism is based on He ii Lyα pumping of the O iii $2p3d\ ^3P^o_2$ (O1 process), we can use the He ii and O iii measurements to obtain approximate constraints on the size of the emitting region and the electron density. As described in § 4.1, we can use the slab model to fit the relative line intensities, thus deriving estimates of the optical depth in the He ii Hα line (λ1640) and the temperature. These values can then be used with the measured O iii λ3133 line intensity to estimate the electron density and size of the emitting region, parameterized in terms of the distance to the source. Additional assumptions include the validity of LTE, an abundance ratio of O iii/He ii equal to the solar value of O/He, and similarly, that He ii/H ii equals the solar value for He/H. For a presumed distance of $\sim$350 pc (based on an estimate of 75 pc for AM Her and assuming comparable luminosities), and following the prescription outlined in equations (7)–(10) of Schachter et al. (1991), we derive $n_{13} \approx 0.04$ and $R_{11} \approx 0.06$, where n_{13} and R_{11} are the electron density (in units of 10^{13} cm^{-3}) and linear scale (in units of 10^{11} cm) of the emitting region. The accuracy of these results, particularly the density, is limited most severely by the wide range of allowable temperatures resulting from our He ii spectral-line analysis.

We can also estimate the size of the line-emitting region from the measured flux of the optically thick emission lines, for which we have an estimate of the line optical depth. The flux in a line is approximately $F = (A_{\rm em}/d^2) \int B_\nu(T)[1 - \exp(-\tau)]d\nu$, where $A_{\rm em}$ is the projected area of the emitting region surface and d is the distance to the source. Using the values of T and τ obtained from our analysis of the He ii line spectrum, and the measured intensity and width of the He ii 1640 Å emission line, we obtain $A_{\rm em} \approx 10^{21.2}$ cm^2, or

$R_{11} \sim 0.03$, for a spherical emission region, which is consistent with the value ($R_{11} \sim 0.06$) we get from the Bowen line spectral analysis.

Since for a ~ 2 hr period system, a $\sim 0.6\, R_\odot$, this suggests then a line-emitting region that is large compared with the white dwarf, and is perhaps about the scale of the L_1 distance. This physical scale for the UV line–emitting region is nominally consistent with the findings of Stockman & Schmidt (1996), i.e., that the UV lines originate in the accretion column and may extend to the L_1 point.

4.2. *Inferred Orbital Inclination*

As previously noted we have very limited phase-sampling in our data, so little information regarding the system binary parameters can be inferred directly from our data. However, it has been pointed out that correlations exist between orbital inclination and UV line strengths in polars, at least for systems with $i \gtrsim 60°$ (la Dous 1991; Friedrich, Staubert, & la Dous 1996). Based on these correlations, we can estimate on the basis of our measurements of the N v, C iv, and Si iv equivalent widths that the inclination of RX J1802.1+1804 is in the approximate 65°–75° range. We have independently investigated the *ROSAT* X-ray light curve, and confirm the earlier report of Griener et al. (1995) that the raw count rates in the PSPC source detection cell reveal a total eclipse of the X-ray emission. This, combined with the low-amplitude modulation in the optical light curve, suggests a high inclination, but probably not greater than $i \sim 75°$. Thus, the inferred inclination from the UV line measurements seems reasonable.

5. CONCLUSIONS

The recently discovered polar RX J1802.1+1804 was observed with *IUE*. It was found to be UV bright, and to have a relatively rich spectrum of emission lines, including multiple species of He ii, carbon, and the O iii Bowen fluorescence lines. In particular, it seems to have an exceptionally large He ii $\lambda 2733 : \lambda 1640$ line-flux ratio among a sample of UV-bright polars in the *IUE* archives. Since this object is further characterized by an unusually soft X-ray spectrum, we searched for possible correlations between the X-ray "softness" parameter and a variety of UV continuum and line properties: we found none other than a weak correlation between He ii $\lambda 2733 : \lambda 1640$ and softness. No phase-dependent information could be obtained from our observations due to inadequate temporal sampling. We have attempted to use the He ii line spectrum, which deviates from a simple nebular recombination spectrum, to derive line optical depths and the temperature of the emitting region. In addition, we have attempted to apply these results to an analysis of the Bowen fluorescence line spectrum to constrain the size and electron density of the emitting region. The resulting size, $R_{11} \approx 0.06$, and density, $n_{13} \approx 0.04$, are not unreasonable, although the accuracy of these calculations is limited by the wide range of allowable temperatures. The application in a comprehensive manner, of a more detailed photoionization code, to CV emission-line spectra, as has recently been attempted by Mauche et al. (1997), is needed for a more complete understanding of the physics and geometry of UV emission-line regions in mCVs. The physical scale that we estimate for the line-emitting region is consistent with the linear scale of the accretion column. This is consistent with recently published results based on phase resolved spectroscopy of other mCVs with the *Hubble Space Telescope*. Our line width measurements, considered in the context of statistical correlations between inclination and UV line widths indicate that we are viewing the system at $\sim 65°$–$75°$, which is consistent with the presence of X-ray eclipsing combined with the absence of visual eclipsing.

We wish to acknowledge the NASA *IUE* Observatory staff for their assistance in carrying out this observing program. In addition, this work made use of the National Space Science Data Archive facility at the NASA Goddard Space Flight Center.

REFERENCES

Beuermann, K., Burwitz, V., Reincsh, K., Schwope, D., & Thomas, H.-C. 1996, in MPE Rep. 263, Röntgenstrahlung from the Universe, ed. H. U. Zimmermann, J. E. Trümper, & H. Yorke (Garching: MPE), 107
Bonnet-Bidaud, J. M., & Mouchet, M. 1988, in A Decade of Astronomy with *IUE* (ESA SP-281; Paris: ESA), 1, 271
Carini, M., Weinstein, D., & Walker, T. 1993, NASA, *IUE* Newsl., 50, 57
Cropper, M. S. 1990, Space Sci. Rev., 54, 195
de Martino, D. 1995, in Cataclysmic Variables, ed. A. Bianchni, M. Delle Valle, & M. Orio (Dordrecht: Kluwer), 397
Friedrich, S., Staubert, R., & la Dous, C. 1996, A&A, 315, 411
Greiner, J., Remillard, R., & Motch, C. 1995, IAU Circ. 6200
Heise, J., & Verbunt, F. 1988, A&A, 189, 112
Kastner, S. O., & Bhatia, A. K. 1996, MNRAS, 279, 1137
la Dous, C. 1991, A&A, 252, 100
Mauche, C. W., Lee, Y. P., & Kallman, T. R. 1997, ApJ, 477, 832
Nichols, J. S., Garhart, M. P., de la Peña, M. D., & Levay, K. L. 1994, NASA *IUE* Newsl. 53
Osterbrock, D. E. 1989, Astrophysics of Gaseous Nebulae and AGN (Mill Valley: University Science Books), 110
Ramsey, G., Mason, K. O., Cropper, M., Watson, M. G., & Clayton, D. L. 1994, MNRAS, 270, 692
Raymond, J. C., Black, J. C., Davis, R. J., Dupree, A. K., Gursky, H., Hartmann, L., & Matilsky, T. A. 1979, ApJ, 230, L95
Schachter, J., Filippenko, A., Kahn, S. M., & Parels, F. B. S. 1991, ApJ, 373, 633
Schmidt, G. D., Szkody, P., Smith, P. S., Silber, A., Tovmassian, G., Hoard, D. W., Gäniscke, B. T., & de Martino, D. 1996, ApJ, 473, 483
Singh, K. P., Barrett, P., Schlegel, E., White, N. E., Szkody, P., Silber, A., Hoard, D. W., & Fierce, E. 1995a, IAU Circ. 6195
Singh, K. P., Barrett, P., White, N. E., Giommi, P., & Angelini, L. 1995b, ApJ, 455, 456
Stockman, H. S., & Schmidt, G. D. 1996, ApJ, 468, 883
Stockman, H. S., Schmidt, G. D., Angel, J. R. P., Liebert, J., Tapia, S., & Beaver, E. A. 1977, ApJ, 217, 815
Szkody, P., Silber, A., Hoard, D. W., Fierce, E., Singh, K. P., Barrett, P., Schlegel, E., & Piirola, V. 1995, ApJ, 455, L43
White, N. E., Giommi, P. & Angelini, L. 1994, BAAS, 185, 4111